V vs SCE). This phenomenon was already noticed by Brunner et al.[14] This large difference is hard to ascribe to solvation and implies a chemical difference in the species in the two solvents.

The electrochemical behavior of A and B^{2+} in dichloromethane is summarized in Scheme II.

Acknowledgment. We thank Prof. Masamoto Iwaizumi and Dr. Minoru Hanaya for the measurement of ESR spectra. The present study was supported by a Grant-in-Aid for Scientific Research, No. 63540469, from the Ministry of Education, Science and Culture, Japan.

Contribution No. 8388 from the Arthur Amos Noyes Laboratories, Division of Chemistry and Chemical Engineering, California Institute of Technology, Pasadena, California 91125

Electrochemical and Spectral Characterization of the "Square Scheme" for the Substitution of *N*-Methylpyrazinium Cation on the Ethylenediaminetetraacetate Complexes of Ruthenium(III) and Ruthenium(II)

Koiti Araki, Ching-Fong Shu, and Fred C. Anson*

Received January 24, 1991

The large difference in the affinity of *N*-methylpyrazinium cations for the ethylenediaminetetraacetate complexes of Ru(II) and Ru(III) produces a pattern of irreversibility in the electrochemical responses exhibited by these complexes. A combination of electrochemical and spectral measurements was utilized to obtain estimates of the equilibrium constants, rate constants, and formal potentials for a "square scheme", which characterizes the behavior of the system.

The replacement of the water molecule on the Ru^{III} center of $Ru^{III}(edta)OH_2^-$ (edta = ethylenediaminetetraacetate) by nitrogen heterocyclic ligands, L, can be readily followed electrochemically because of the shift in the formal potential of the Ru^{III}/Ru^{II} couple, which results from the substitution.[1,2] The unusual lability of the H_2O molecule coordinated to $Ru^{III}(edta)OH_2^-$[1,4] facilitates its replacement by ligands with greater affinities for Ru(III). The usual pattern is for the reversible couple $Ru^{III}(edta)OH_2^-/Ru^{II}(edta)OH_2^{2-}$ to be replaced by a new, reversible couple, $Ru^{III}(edta)L/Ru^{II}(edta)L$. However, in cases where the incoming ligand is bound only weakly to Ru(III) but much more strongly to Ru(II), an irreversible or quasi-reversible pattern can be encountered.[2,5,6] A particularly clear example of this type of behavior is provided by the interaction between $Ru^{III}(edta)OH_2^-$ and the strongly π-accepting *N*-methylpyrazinium cation (NMP^+). As is demonstrated in this report, the system adheres to the "square scheme" shown in Scheme I. The value of K_1 is much smaller than K_2 so that $E^f_{NMP} > E^f_{H_2O}$. Values of the two equilibrium constants and formal potentials as well as estimates of the rate constants governing the ligand-exchange reactions at the Ru(edta) center are given in this report. The values of the parameters obtained are consistent with the generally understood chemistry of the +3 and +2 oxidation states of Ru in which σ-acceptance and π-back-donation are important factors that influence the coordination of ligands to Ru(III) and Ru(II), respectively.

Experimental Section

Materials. $Ru(Hedta)\cdot 4H_2O$ was synthesized according to Mukaida et al.[7] from H_4edta and $RuCl_3\cdot nH_2O$. *N*-Methylpyrazinium hexafluorophosphate was prepared by metathesis from the commercially available iodide and was recrystallized three times from water. Other chemicals were analytical grade and were used as received. Glassy carbon electrodes (Tokai Chemical Co., Tokyo) were mounted with heat-shrinkable tubing as previously described.[8]

Scheme I

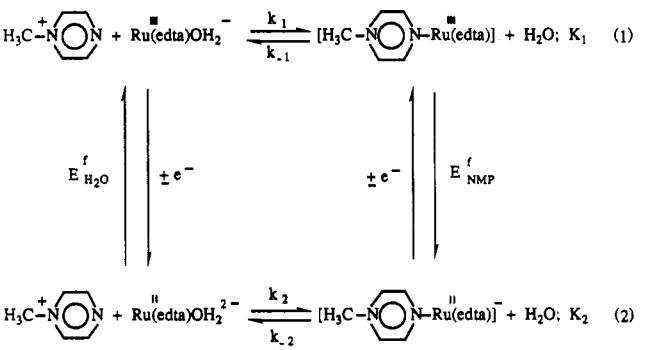

Apparatus and Procedures. Spectra were obtained with a Hewlett Packard 8450A spectrophotometer and 7225A plotter. Cyclic and rotating ring–disk voltammetry and normal pulse polarography were carried out with conventional instruments and two compartment cells. The rotating gold-disk–platinum-ring electrode (Pine Instrument Co.) had the following dimensions: r_1 = 0.38 cm; r_2 = 0.40 cm; r_3 = 0.42 cm. Glassy-carbon electrodes were polished first with 0.3-μm alumina followed by 0.05-μm alumina to produce a mirror-like finish. Polished electrodes were sonicated in pure water to remove residual alumina from their surfaces. Potentials were measured with respect to a Ag/AgCl (KCl = 1.0 M) reference electrode but are reported versus the standard saturated calomel electrode (SCE). All experiments were conducted at the ambient laboratory temperature, 22 ± 2 °C.

Results and Discussion

Reaction of $Ru^{III}(edta)OH_2^-$ with *N*-Methylpyrazinium Cations. The most labile form of the $Ru^{III}(edta)OH_2^-$ complex is present at pH values where the single uncoordinated carboxylate group is ionized.[1,2] The pK_A of this carboxylic acid is 2.4;[1,7] our experiments were carried out in acetate buffer solutions near pH 4.5. Solutions of $Ru^{III}(edta)OH_2^-$ (0.2 mM) are faintly yellow at pH 4.5, but addition of *N*-methylpyrazinium (NMP^+) produces the immediate development of an intense orange color. The color change is the result of a broad absorption between 500 and 420

(1) Matsubara, T.; Creutz, C. *J. Am. Chem. Soc.* **1978**, *100*, 6255; *Inorg. Chem.* **1979**, *18*, 1956.
(2) Toma, H. E.; Santos, V. S.; Mattioli, M. V. D.; Oliveira, L. H. A. Polyhedron **1987**, *6*, 603.
(3) Bajaj, H. C.; van Eldik, R. *Inorg. Chem.* **1988**, *27*, 4052; **1989**, *28*, 1980; **1990**, *29*, 2855.
(4) Ogino, H.; Shimura, M. *Adv. Inorg. Bioinorg. Mech.* **1986**, *4*, 107.
(5) Elliott, M. G.; Zhang, S.; Shepherd, R. E. *Inorg. Chem.* **1989**, *28*, 3036.
(6) Toma, H. E.; Araki, K. Submitted for publication in *J. Coord. Chem.*
(7) Mukaida, M.; Okuno, H.; Ishimori, T. *Nippon Kagaku Zasski* **1965**, *86*, 589.
(8) Oyama, N.; Anson, F. C. *J. Am. Chem. Soc.* **1979**, *101*, 3450.

0020-1669/91/1330-3043$02.50/0

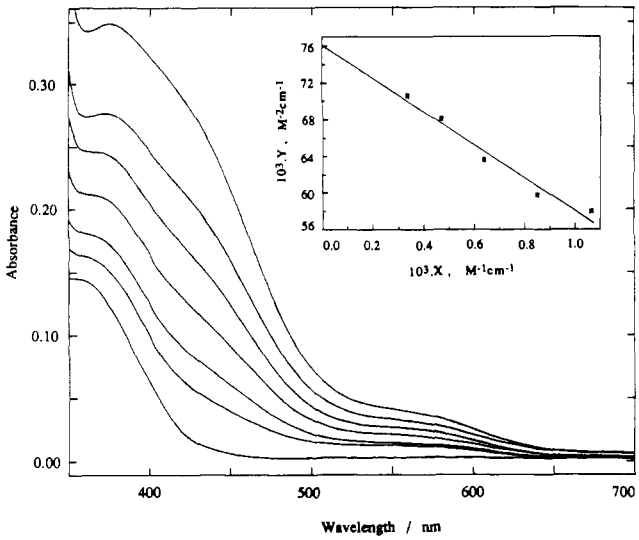

Figure 1. Absorption spectra of mixtures of 0.2 mM $Ru^{III}(edta)OH_2^-$ with *N*-methylpyrazinium cations (NMP^+). The concentrations of NMP^+ from the bottom to the top spectrum were 0, 3.1, 5.1, 8.2, 12, 16, 20.4 mM. Supporting electrolyte was 0.2 M CF_3COONa + 0.05 M acetate buffer (pH 4.6). Optical path length was 1 cm. The inset shows the spectral evaluation of the equilibrium constant for reaction 1 by the method of Newton and Arcand.[9] The data points were obtained at 420 nm. For the abscissa, X is the difference between the measured absorbances of the Ru(III)–NMP^+ mixture and the absorbance of the NMP^+ ligand alone (negligible in our experiment) divided by the total concentration of Ru(III). For the ordinate, Y is X minus the molar absorbtivity of $Ru^{III}(edta)OH_2^-$ divided by the concentration of uncoordinated NMP^+. The slope of the linear plot is the equilibrium constant.

nm (Figure 1). The weak absorption centered near 560 nm in Figure 1 resembles the spectrum of the reduced $[Ru^{II}(edta)NMP]^-$ complex (Figure 4). The intensity of this absorption increases slowly with time in the absence of any intentionally added reducing agent. It may result from a slow reaction in which the edta ligand is oxidized. We did not pursue this aspect of the reaction between $Ru^{III}(edta)OH_2^-$ and NMP^+.

The cyclic voltammetry of $Ru^{III}(edta)OH_2^-$ in the absence of coordinating ligands is shown in Figure 2A. An uncomplicated, reversible response is obtained that is independent of the initial potential of the electrode, and cathodic current begins to flow near −0.1 V. A very different response is obtained in the presence of NMP^+ (Figure 2B). The initial potential must be positive of 0.35 V to avoid the flow of cathodic current, and the voltammogram consists of two sets of waves: The first, small, cathodic wave near 0.35 V is plateau-shaped instead of peaked and increases less rapidly with scan rate than the second, peaked wave near −0.25 V. These features are the hallmarks of a system in which the kinetics of a chemical reaction preceding the electrode reaction controls the magnitude of the first, plateau-shaped cathodic wave. Reaction 1 in Scheme I is the likely current-controlling reaction. The second cathodic peak in Figure 2B corresponds to the reduction of $Ru^{III}(edta)OH_2^-$, and the resulting $Ru^{II}(edta)OH_2^{2-}$ engages in reaction 2 in Scheme I. This ligand-exchange reaction is evidently reasonably rapid because only at the highest scan rate is there a small anodic peak corresponding to the oxidation of unreacted $Ru^{II}(edta)OH_2^{2-}$. The primary anodic peak appears at the potential where the first small cathodic plateau appeared, and it is therefore attributable to the oxidation of the $[Ru^{II}(edta)NMP]^-$ complex.

When the initial potential of the electrode is held at −0.35 for 60 s to reduce the $Ru^{III}(edta)OH_2^-$ in the vicinity of the electrode to $Ru^{II}(edta)OH_2^{2-}$, scans to more positive potentials produce the response shown in Figure 2C. There is almost no anodic current at the potential where $Ru^{II}(edta)OH_2^{2-}$ is oxidized. A large anodic peak corresponding to the oxidation of $[Ru^{II}(edta)NMP]^-$ is present near 0.3 V, but most of the oxidized product is not reduced at potentials near those where it is generated. The $Ru^{III}(edta)$-NMP generated at 0.3 V is apparently largely dissociated by the

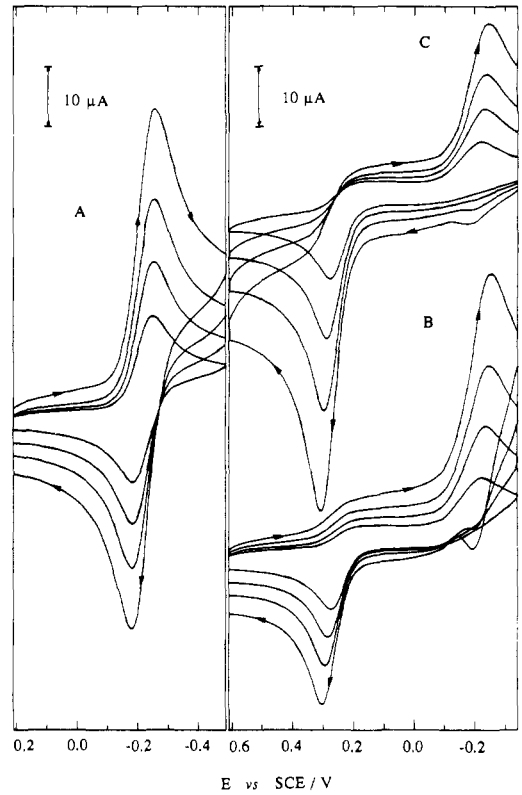

Figure 2. Cyclic voltammetry of 0.72 mM $Ru^{III}(edta)OH_2^-$ in the absence and presence of NMP^+: (A) scans in the absence of NMP^+ (initial potential = 0.2 V; scan rates were 20, 50, 100, and 200 mV s^{-1}); (B) repeat of A in the presence of 0.7 mM NMP^+ (initial potential = 0.6 V); (C) repeat of B except the electrode was held at −0.35 V for 60 s before the potential was scanned to more positive values.

time the electrode potential is scanned to values where it could be reduced, and the primary cathodic peak corresponds to the reduction of $Ru^{III}(edta)OH_2^-$. Thus, the stable forms of the Ru(edta) complexes in the presence of NMP^+ are those shown in the upper left and lower right hand corners of Scheme I and the unstable forms of the complexes occupy the other two corners.

Characterization of Reaction 1. The spectral changes produced when NMP^+ is mixed with $Ru^{III}(edta)OH_2^-$ (Figure 1) can be utilized to estimate K_1, the equilibrium constant for the replacement of the H_2O in $Ru^{III}(edta)OH_2^-$ by NMP^+ (reaction 1). The method employed is due to Newton and Arcand.[9] The absorbances at 420 nm of various mixtures of $Ru^{III}(edta)OH_2^-$ and NMP^+ were measured, and the plot shown in the inset in Figure 1 was prepared. From the slope of the least-squares line through the data points, a value of 18 M^{-1} was calculated for K_1. (The ratio of the slope to the intercept of the plot leads to 3.7×10^3 M^{-1} cm^{-1} as the molar absorbance at 420 nm of the Ru^{III}-(edta)NMP complex.) Similar plots of data obtained at 400 and 440 nm produced slopes of 17 and 22 M^{-1} so the resulting average value of K_1 is 19 M^{-1}.

The rate at which the $Ru^{III}(edta)NMP$ complex spontaneously dissociates into $Ru^{III}(edta)OH_2^-$ and NMP^+ is governed by the rate constant k_{-1} (Scheme I). This rate constant was evaluated by voltammetric measurements with a rotating ring–disk electrode:[10] A solution of $[Ru^{II}(edta)NMP]^-$ was prepared from a mixture of $Ru^{III}(edta)OH_2^-$ and NMP^+ by reduction with zinc amalgam under argon. The oxidation of the $[Ru^{II}(edta)NMP]^-$ complex at the disk electrode at 0.27 V produced the unstable $Ru^{III}(edta)NMP$ complex, which partially decomposed during the time required for it to be swept from the disk to the ring electrode.

(9) Newton, T. W.; Arcand, G. M. *J. Am. Chem. Soc.* **1953**, *75*, 2449. Cf.: Rossotti, J. C. *The Determination of Stability Constants*; McGraw Hill: New York, 1961; p 275.

(10) Albery, W. J.; Hitchman, M. L. *Ring-Disc Electrodes*; Clarendon Press: Oxford, 1971.

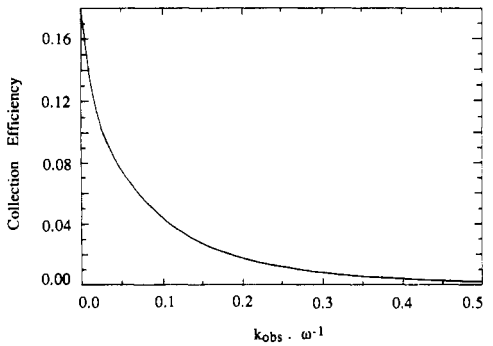

Figure 3. Variation of collection efficiency with the rate constant governing the first-order, irreversible decomposition of a product generated at the disk electrode (e.g., k_{-1} in Scheme I) for a rotating ring–disk electrode having the dimensions given in the Experimental Section. The curve was calculated from equations given in ref 10. For collection efficiencies between 0.08 and 0.14 manual extrapolation of the curves calculated for larger and smaller collection efficiencies was employed because of difficulties in matching the computer-calculated values within this range. Numerical parameters employed in calculating the curve were as follows: reactant diffusion coefficient = 5×10^{-6} cm^2 s^{-1}; kinematic viscosity = 0.01 cm^2 s^{-1}. The units of ω are rad s^{-1}.

The ring was maintained at 0.0 V where the undecomposed Ru^{III}(edta)NMP complex was reduced but the Ru^{III}(edta)OH_2^- complex was not (Figure 2B). The ratio of the ring to disk currents, i.e., the collection efficiency,[10] was measured as a function of the rate of rotation of the ring–disk electrode to evaluate k_{-1}. The procedure involved the use of a working curve calculated from equations derived by Albery and Hitchman,[10-12] which relate measured collection efficiencies to the rate constant for the first-order, irreversible decomposition of species generated at the disk electrode. The working curve calculated for the rotating ring–disk electrode employed in this study is shown in Figure 3. The computer program employed to obtain this curve was checked by verifying that it reproduced the curves given in Figure 9.1 of ref 10. The rate constant for the reverse of reaction 1 in Scheme I was so large that rotation rates above 5000 rpm were required to obtain measurable ring currents. As a result, only a limited set of data could be obtained (Table IA) from which an average value of $k_{-1} = 2 \times 10^2$ s^{-1} resulted.

To assure that the rotating ring–disk methodology employed was reliable, we applied the same approach to measure the rate of dissociation of the corresponding acetonitrile (AN) complex, Ru^{III}(edta)AN^-. The rate of this dissociation reaction is considerably slower so that larger collection efficiencies could be obtained over a wide range of rotation rates. The results, summarized in Table IB, lead to a rate constant of 2.4 s^{-1}, which is in good agreement with the value of 3.2 s^{-1} measured by Matsubara and Creutz in stopped-flow experiments.[1] Thus, the reliability of the working curve in Figure 3 was verified.

The large separation between the two cathodic responses in Figure 2B allowed the rate of the forward direction of reaction 1 in Scheme I to be investigated by chronoamperometry in the form of normal pulse voltammetry.[13] We carried out such experiments to determine if the resulting value of k_1 was compatible with that calculated from the values of K_1 and k_{-1} estimated in the spectral and rotating ring–disk electrode experiments. Normal pulse voltammograms were recorded for solutions of Ru^{III}(edta)OH_2^- to which increasing quantities of NMP^+ were added. The initial electrode potential was 0.4 V, and it was stepped to increasingly negative values. The magnitudes of the plateau currents for the first cathodic wave, corresponding to the reduction of the Ru^{III}(edta)NMP complex present at equilibrium plus that generated at the surface of the electrode by reaction 1, were measured at ca. 0.15 V. The results were not analyzed in the usual way[14a] by means of the equation of Koutecky and Brdicka[14b] because it was derived for the case where a negligible quantity of the electroactive reactant is present in the test solution at equilibrium. The average value of K_1 estimated as in Figure 1 (K_1 = 19 M^{-1}) was too large to be compatible with this condition for the concentrations of NMP^+ we employed to produce kinetic currents large enough for convenient measurement. We therefore employed the more general equation of MacDonald,[15] which is applicable to cases, such as the present one, where substantial

Table I

A. Estimation of k_{-1} (Scheme I) by Rotating Ring–Disk Voltammetry[a]

ω,[b] rpm	N_k[c]	$10^{-2}k_{-1}$,[d] s^{-1}
5000	0.0057	185
5750	0.0063	206
6000	0.0072	204
		av 200

B. Repeat of the Experiments of Part A Using Acetonitrile in Place of NMP^+[e]

ω, rpm	N_k	k_{-1},[f] s^{-1}
500	0.069	2.9
750	0.095	2.4
1000	0.106	2.6
1600	0.126	2.4
2500	0.15	2.0
3000	0.15	2.1
4000	0.16	2.4
5000	0.16	2.4
		av 2.4

[a] The solution contained 1 mM NMP^+, 0.2 M CF_3COONa, and 0.05 M acetate buffer (pH 4.6). The disk potential was scanned from 0 to 0.5 V with the ring potential maintained at 0 V. Just before the experiment, sufficient Ru^{II}(edta)OH_2^{2-} (prepared by reduction of Ru^{III}edtaOH_2^- with zinc amalgam under argon) was added to the solution to produce a 1 mM solution of [Ru^{II}edtaNMP]$^-$. [b] Electrode rotation rate. [c] Collection efficiency = ring current/disk current. [d] Obtained from the working curve in Figure 4 by taking the diffusion coefficient of Ru^{III}(edta)NMP to be 5×10^{-6} cm^2 s^{-1}. [e] The solution was prepared as in part A except that the concentrations of [Ru^{II}(edta)OH_2^{2-}] and acetonitrile were both 0.21 mM. [f] Rate Constant for the reaction $Ru^{III}(edta)AN^- + H_2O \rightarrow Ru^{III}(edta)OH_2^- + AN$ (AN ≡ acetonitrile).

Table II. Chronoamperometeric (Normal Pulse Voltammetric) Evaluation of k_1 in Scheme I[a]

[NMP^+], mM	[Ru^{III}(edta)OH_2^-], mM	i_k,[b] μA	$10^{-3}k_1$,[c] M^{-1} s^{-1}	K_1, M^{-1}
0	0.2	0		
4.4	0.1	4.1	3.5	18
5.3	0.2	8.7	3.1	16
8.7	0.1	5.6	2.6	13
12.1	0.2	15.0	3.0	15
19.1	0.2	18.1	2.7	14
			av 3.0	av 15

[a] The normal pulse voltammetric parameters were as follows: pulse width, 2 s; sample width, 17 ms; effective time of current sampling, 41.5 ms; [Ru^{III}(edta)OH_2^-] = 0.2 mM; supporting electrolyte, 0.2 M CF_3COONa + 0.05 M acetate buffer (pH 4.6). [b] Normal pulse plateau current measured at 0.15 V. [c] Evaluated by adjusting k_1 to obtain the best agreement with eq 4.221 of ref 15 using $k_{-1} = 2 \times 10^2$ s^{-1}.

(11) Albery, W. J.; Hitchman, M. L.; Ulstrup, J. *Trans. Faraday Soc.* **1968**, *64*, 2831.
(12) The equations and numerical coefficients employed are given in Chapter 3, Chapter 9, and Appendix 5 of ref 10. To cover the entire range of collection efficiencies involved, eqs 3.12, 3.13, 9.4, 9.5, 9.6, 9.8, 9.9, and 9.10 were utilized. A computer program from which working curves for particular values of the disk, gap, and ring dimensions were obtained is available upon request.
(13) Bard, A. J.; Faulkner, L. R. *Electrochemical Methods*; John Wiley, Inc.: New York, 1980; p 186.
(14) (a) Reference 13, p 444. (b) Koutecky, J.; Brdicka, R. *Collect. Czech. Chem. Commun.* **1947**, *12*, 337.
(15) Macdonald, D. D. *Transient Techniques in Electrochemistry*, Plenum Press: New York, 1977, p 98.

Table III. Rate Constants, Equilibrium Constants and Formal Potentials for the Components of the Square in Scheme I

reaction 1	$k_1 = (3\text{–}4) \times 10^3$ M^{-1} s^{-1}	$k_{-1} = 2 \times 10^2$ s^{-1}	$K_1 = 15\text{–}19$ M^{-1}
reaction 2	$k_2 < 5.6 \times 10^3$ M^{-1} s^{-1}	$k_{-2} < 1.1 \times 10^{-7}$ s^{-1}	$K_2 = \sim 5 \times 10^{10}$ M^{-1}
	$E^f_{H_2O} =$ −0.24 V vs SCE	$E^f_{NMP} =$ 0.31 V vs SCE	

quantities of the electroactive complex are present at equilibrium. The rather complicated equation involved does not lend itself to the calculation of simple working curves so the data were fitted to the equation by setting $k_{-1} = 2 \times 10^2$ s^{-1} and varying k_1 to obtain the best agreement. The results, shown in Table II, lead to an average value of 3×10^3 M^{-1} s^{-1} for k_1, which corresponds to a value of 15 M^{-1} for K_1. These values for k_1 and K_1 are sufficiently close to those obtained from the rotating ring–disk and spectrophotometric experiments ($k_1 = 4 \times 10^3$ M^{-1} s^{-1}; $K_1 = 19$ M^{-1}) to regard the parameters characterizing reaction 1 to be reasonably well estimated as summarized in the first line of Table III.

Characterization of Reaction 2. The equilibrium constant for reaction 2 in Scheme I can be evaluated from eq 3, where the

$$(RT/F) \ln K_2 = E^f_{NMP} - E^f_{H_2O} + (RT/F) \ln K_1 \quad (3)$$

formal potentials $E^f_{H_2O}$ and E^f_{NMP} correspond to the half-reactions specified in Scheme I and K_1 is the equilibrium constant for reaction 1. $E^f_{H_2O}$ was measured as −0.24 V vs SCE in the supporting electrolyte employed. To evaluate E^f_{NMP}, it was necessary to take into account the instability of the Ru^{III}(edta)NMP complex. The anodic peak potentials in the cyclic voltammograms in Figure 2B, C are related to E^f_{NMP} according to the relationships derived by Nicholson and Shain for electrode reactions resulting in products that undergo subsequent chemical reactions.[16] Application of the working curve in ref 16 for irreversible decomposition reactions to the voltammograms in Figure 2C led to E^f_{NMP} = 0.31 V vs SCE. From this value of E^f_{NMP}, the value of K_2 calculated from eq 3 is 4×10^{10} M^{-1}.

K_2 was also evaluated spectrophotometrically by adding $Ru^{II}(edta)OH_2^{2-}$ to solutions containing NMP^+ and dimethyl sulfoxide (dmso), which also forms a strong complex with Ru^{II}(edta) with a known formation constant ($K_{dmso} = 7.7 \times 10^9$ M^{-1}).[6] $Ru^{III}(edta)OH_2^-$ was also added to the mixture to serve as an electron-exchange catalyst for the equilibration of the Ru^{II}(edta) with the two competing ligands because the ligand-exchange reactions proceed much more rapidly with $Ru^{III}(edta)OH_2^-$ than with $Ru^{II}(edta)OH_2^{2-}$. The addition of $Ru^{II}(edta)OH_2^{2-}$ to the mixture of the two ligands produced an immediate intense color, which decreased for a few minutes until a stable spectrum was obtained with a maximum at 560 nm corresponding to the $[Ru^{II}(edta)NMP]^-$ complex. In Figure 4 are shown a set of equilibrium spectra obtained with varying ratios of dmso to NMP^+. $Ru^{II}(edta)dmso^{2-}$ does not absorb at 560 nm so the measured absorptions in Figure 4 are expected to obey eq 4, where Abs° and Abs are the absorbances measured in the

$$\frac{Abs^\circ}{Abs} = \frac{K_{dmso}}{K_{NMP}} \frac{[dmso]}{[NMP^+]} + 1 \quad (4)$$

absence and presence of dmso, respectively, and K_{dmso} and K_{NMP} are the equilibrium formation constants for the indicated $[Ru^{II}(edta)L]^{2-}$ complex. A plot of Abs°/Abs vs the ratios of the concentrations of the uncoordinated ligands is shown in Figure 5A. The data define a good straight line with the expected intercept and a slope, 0.14, from which K_{NMP} was calculated as 5.4×10^{10} M^{-1}. This constant is in good agreement with the value for K_2 obtained from the cyclic voltammetric data, 4.0×10^{10} M^{-1}.

The data in Figure 5B were obtained in the same type of experiment when the NMP^+ ligand was replaced with pyrazine (pyz). The slope of the line, 51, is in reasonable agreement with

(16) Nicholson, R. S.; Shain, I. *Anal. Chem.* **1964**, *36*, 706. The published results are for reductions but conversion to oxidations requires only appropriate changes in signs.

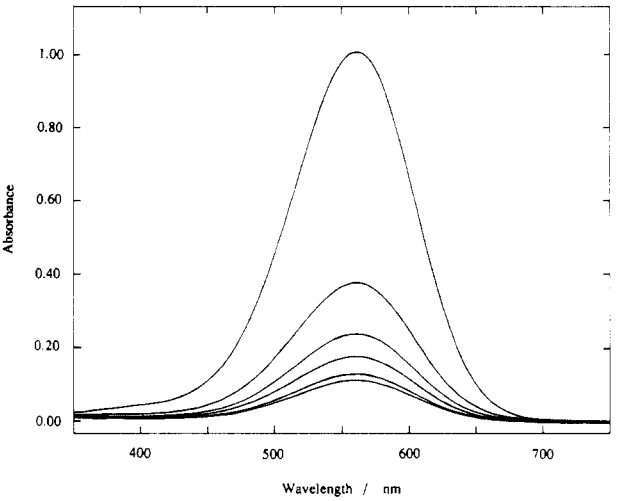

Figure 4. Absorption spectra of solutions containing 0.05 mM $Ru^{II}(edta)OH_2^{2-}$, 0.01 mM $Ru^{III}(edta)OH_2^-$, 0.2 mM NMP^+, and various concentrations of dmso in 0.05 M acetate buffer (pH 4.8). Concentrations of dmso from top to bottom: 0, 2.4, 4.8, 7.3, 9.7, 12 mM. Spectra were recorded after the absorption decreased to its steady value about 10 min after the $Ru^{II}(edta)OH_2^{2-}$ was added to a deoxygenated mixture of the other ingredients.

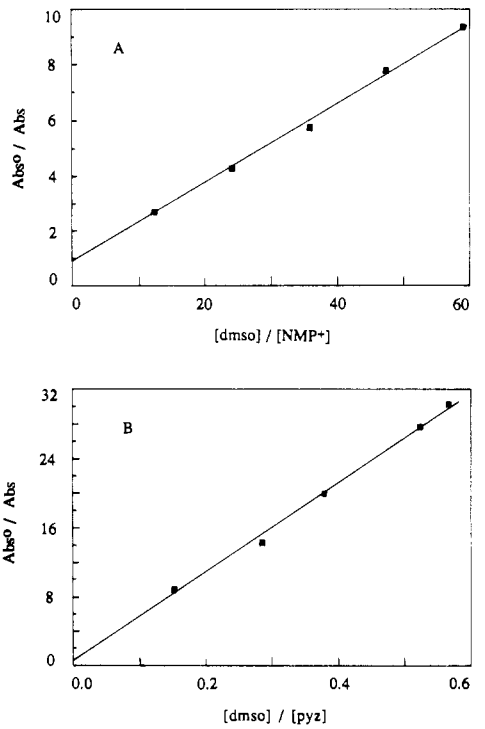

Figure 5. Plots of spectral data for mixtures of $Ru^{II}(edta)L$ complexes (L = NMP^+, dmso, pyrazine) according to eq 4: (A) mixtures of dmso and NMP^+; (B) mixtures of dmso and pyrazine (pz).

the ratio of the reported values of $K_{dmso} = 7.7 \times 10^9$ M^{-1} [6] and $K_{pyz} = 1.7 \times 10^8$ M^{-1},[1] $K_{dmso}/K_{pyz} = 45$, which confirms the reliability of the procedure employed to measure $K_{NMP} = K_2$ in Figure 5A.

The value of k_2 (or k_{-2}) is needed in order to complete the characterization of reaction 2 in Scheme I. Electrochemical methods for measuring k_2 (or k_{-2}), such as the rotating ring–disk electrode technique employed to evaluate k_{-1}, are not suitable because the Ru^{III}(edta) present in the diffusion layer at the surface of monitoring electrodes acts as a catalyst for ligand-exchange reactions such as reaction 2 by means of rapid electron exchange between the more rapidly formed Ru^{III}edta L complex (L = an incoming ligand) and the less reactive $Ru^{II}(edta)OH_2^{2-}$ complex.[1] Instead, we attempted to obtain an estimate of k_2 by the method of concurrent reactions.[17] The initial distribution of complexes

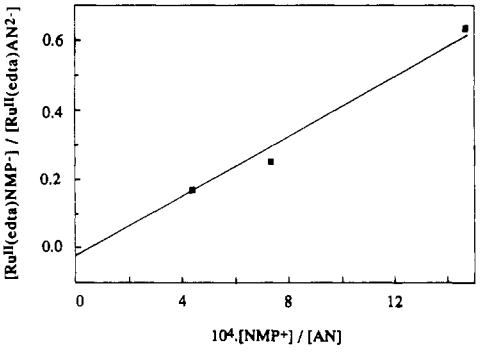

Figure 6. Estimation of k_2 (Scheme I) from the initial distribution of complexes formed in the concurrent reaction of $Ru^{II}(edta)OH_2^{2-}$ with NMP^+ and acetonitrile (AN).

that resulted when $Ru^{II}(edta)OH_2^{2-}$ was reacted with a mixture of acetonitrile and NMP^+ was determined spectroscopically. The kinetics of the substitution of these two ligands on $Ru^{II}(edta)OH_2^{2-}$ can be made competitive by adjusting their relative concentrations. The initial concentrations of $Ru^{II}(edta)NMP^-$ produced in the reactions of such mixtures were substantially less than the equilibrium concentrations calculated from the known equilibrium constants. The rates of the dissociation of the $Ru^{II}(edta)AN^{2-}$ and $[Ru^{II}(edta)NMP]^-$ complexes are low enough to allow the spectra of solutions of the mixtures to be measured (usually within 1 min) before they are altered by the slow ligand-exchange reactions that eventually produce the equilibrium mixture. A plot of $[Ru^{II}(edta)NMP^-]/[Ru^{II}(edta)AN^{2-}]$ vs $[NMP^+]/[AN]$ is shown in Figure 6. It is reasonably linear with a slope of 4.3×10^2. Since the rate constant for substitution on $Ru^{II}(edta)OH_2^{2-}$ by acetonitrile is 13 M^{-1} s^{-1},[1] the value of k_2 calculated from the slope of the line in Figure 6 is 5.6×10^3 M^{-1} s^{-1}. This is an unusually large rate constant for substitution on $Ru^{II}(edta)OH_2^{2-}$.[1] However, the rate of substitution on $Ru^{II}(edta)OH_2^{2-}$ by a cationic ligand would be expected to be enhanced by electrostatic factors. For example, rate constants for substitution on the related $Fe(CN)_5OH_2^{3-}$ complex by cationic ligands tend to be 5–50-fold larger than those for neutral ligands. In particular, the rate constant for NMP^+ is 7-fold larger than that for pyrazine.[18]

The estimate obtained for k_2 may also have been enhanced because of catalysis of the measured rates by the presence of residual $Ru^{III}(edta)OH_2^-$ despite our best efforts to reduce the solutions of $Ru^{III}(edta)OH_2^-$ completely with zinc amalgam. Matsubara and Creutz[1] emphasized the difficulties in avoiding such catalysis, and the problem is more severe in the case of NMP^+ because this ligand can serve as an outer-sphere oxidant of $Ru^{II}(edta)OH_2^{2-}$. (The formal potential of the NMP^+/NMP couple at pH 4.5 is ca. −0.48 vs. SCE,[19] which is only 0.24 V more negative than that of the $Ru(edta)OH_2^{-/2-}$ couple.) Thus, the value of k_2 obtained from the concurrent reaction experiments is best regarded as an upper limit on the value of this rate constant.

Comparisons of *N*-Methylpyrazinium and Pyrazine Complexes of Ru(edta). The set of equilibrium and kinetic constants evaluated for the reactions in Scheme I (Table III) provides a basis for comparing cationic *N*-methylpyrazinium and neutral pyrazine as ligands which exhibit affinity for $Ru^{III}(edta)$ and $Ru^{II}(edta)$. The strong absorption band at 560 nm ($\epsilon_{560} = 19.4 \times 10^3$ M^{-1} cm^{-1}) in the spectrum of $Ru^{II}(edta)NMP^-$ (Figure 4) is attributable to a metal-to-ligand $d\pi-p\pi^*$ charge-transfer transition. The band maximum appears at lower energy than that for the corresponding pyrazine complex ($\lambda_{max} = 463$ nm; $\epsilon_{463} = 11.6 \times 10^3$ M^{-1} cm^{-1}[1]). This shift to the red is in the direction expected because the positive charge of the NMP^+ cation increases the π-acceptor and decreases the σ-donor character of the ligand. Similar comparisons were offered by Diamantis and Dubrawski.[20]

The equilibrium constant governing the coordination of NMP^+ to $Ru^{III}(edta)$, K_1, is ca. 500 times smaller than the corresponding constant in the case of pyrazine.[1] Since back-bonding is much less significant for Ru(III) than for Ru(II), the decreased affinity of NMP^+ for $Ru^{III}(edta)$ reflects the diminished σ-donating capacity of the cationic ligand. The value of k_1 (Scheme I) is only ca. 2 times smaller than the corresponding rate constant for the pyrazine complex[1] so the primary effect resulting from the diminished σ-donation of NMP^+ is an enhancement in the rate of its dissociation from the $Ru^{III}(edta)$ center.

Matsubara and Creutz,[1] who examined the kinetics of the formation and dissociation of several $Ru^{III}(edta)$ complexes with neutral ligands, observed a slope near 0.5 in logarithmic plots of the rate constants vs the equilibrium constants for substitution on the $Ru^{III}(edta)OH_2^-$ complex. A much smaller value of k_1 (than the measured value of 3×10^3 M^{-1} s^{-1}) would be expected if the NMP^+ ligand followed the same trend reported by Matsubara and Creutz.[1] The larger value of k_1 we observed is probably a reflection of the cationic nature of NMP^+, which results in a larger value of the (unmeasured) equilibrium constant for the formation of the precursor complex and, therefore, of the observed rate constant.

Acknowledgment. This work was supported by the National Science Foundation. K.A. was the grateful recipient of a grant from the University of Sao Paulo/Interamerican Bank for Development.

(17) Espenson, J. H. *Chemical Kinetics and Reaction Mechanisms*; McGraw-Hill: New York, 1981; p 57.
(18) Macartney, D. H. *Rev. Inorg. Chem.* **1988**, *9*, 101.
(19) Toma, H. E.; Chagar, H. C. *An. Acad. Brasil. Ciênc.* **1978**, *50*, 487.
(20) Diamantis, A. A.; Dubrawski, J. V. *Inorg. Chem.* **1981**, *20*, 1142.